Clinical Imaging 119 (2025) 110417

Contents lists available at ScienceDirect

Clinical Imaging

journal homepage: www.elsevier.com/locate/clinimag

Body Imaging

Colorectal liver metastases on gadoxetic acid-enhanced MRI: Typical characteristics decrease after chemotherapy

Denise J. van der Reijd [a,b,*], Ezgi A. Soykan [a,c], Birthe C. Heeres [a], Doenja M.J. Lambregts [a,b], Marieke A. Vollebergh [d], Koert F.D. Kuhlmann [e], Niels F.M. Kok [e], Petur Snaebjornsson [f,g], Regina G.H. Beets-Tan [a,h], Monique Maas [a,b], Elisabeth G. Klompenhouwer [a]

[a] Department of Radiology, Antoni van Leeuwenhoek – The Netherlands Cancer Institute, Amsterdam, the Netherlands
[b] GROW School for Oncology and Reproduction, Maastricht University, Maastricht, the Netherlands
[c] Department of Radiology and Nuclear Medicine, Cancer Center Amsterdam, Amsterdam UMC, University of Amsterdam, Amsterdam, the Netherlands
[d] Department of Gastrointestinal Oncology, Antoni van Leeuwenhoek – The Netherlands Cancer Institute, Amsterdam, the Netherlands
[e] Department of Surgical Oncology, Antoni van Leeuwenhoek – The Netherlands Cancer Institute, Amsterdam, the Netherlands
[f] Department of Pathology, Antoni van Leeuwenhoek – The Netherlands Cancer Institute, Amsterdam, the Netherlands
[g] Faculty of Medicine, University of Iceland, Reykjavik, Iceland
[h] Institute of Regional Health Research, University of Southern Denmark, Odense, Denmark

ARTICLE INFO

Keywords:
Magnetic resonance imaging
Liver
Colorectal cancer
Metastasis
Gadoxetic acid
Chemotherapy

ABSTRACT

Purpose: To determine to what extent colorectal liver metastases (CRLM) display typical imaging characteristics on gadoxetic acid-enhanced magnetic resonance imaging (MRI) and what changes after chemotherapy.
Methods: We retrospectively identified 258 patients with a gadoxetic acid-enhanced MRI between 2015 and 2021 and pathologically proven non-mucinous adenocarcinoma CRLM. 722 unique CRLMs were analyzed: 378 CRLM in only the chemotherapy-naïve analysis; 217 in post-chemotherapy analysis; and 127 CRLM were analyzed both pre- and post-chemotherapy. The following six characteristics were defined as typical; "hypovascular", "unenhanced T1-weighted (UE-T1W) hypointensity", "arterial rim enhancement", "non-enhancing during hepatobiliary phase", "T2-weighted (T2W) mild hyperintensity", and "diffusion restriction".
Results: All six typical characteristics were found in 249/505 chemotherapy-naïve CRLM (49 %) and 87/344 post-chemotherapy CRLM (25 %). The occurrence of some typical characteristics decreased post-chemotherapy: UE-T1W hypointensity 485/505 (96 %) versus 311/336 (93 %), arterial rim enhancement 291/498 (58 %) versus 154/301 (51 %), T2W mild hyperintensity 478/505 (95 %) versus 269/338 (79 %), and diffusion restriction 435/497 (87 %) versus 200/306 (65 %). Almost all metastases showed a hypovascular appearance, both in the chemotherapy-naïve (495/504, 98 %) and post-chemotherapy group (330/331, 100 %). Additionally, all CRLM appeared non-enhancing compared to the liver in the hepatobiliary phase (100 %).
Conclusion: Most CRLM show various combinations of at least five typical characteristics on gadoxetic acid-enhanced MRI. Arterial rim enhancement is the least prevalent characteristic both in chemotherapy-naïve and post-chemotherapy patients. Post-chemotherapy the occurrence of typical MRI characteristics decreases, especially mild T2W hyperintensity and the presence of diffusion restriction.

1. Introduction

About 25–30 % of colorectal cancer patients develop liver metastases, impairing survival rates significantly.[1–3] Over the last decades, the treatment options for colorectal liver metastases (CRLM) have improved resulting in better prognostic outcomes.[4] Chemotherapy has a key role in the treatment of CRLM, not solely in palliative settings, but also as a neoadjuvant treatment for patients with unfavorable risk factors, or with the aim to downsize initially unresectable CRLM. As a consequence, accurate diagnosis of liver lesions in colorectal cancer patients has become pivotal for tailored treatment planning.

Multiple imaging modalities are used for the diagnosis of CRLM, such as computed tomography (CT), ultrasound, positron emission tomography, and magnetic resonance imaging (MRI). MRI has the highest

* Corresponding author at: Plesmanlaan 121, 1066CX Amsterdam, the Netherlands.
E-mail address: denisevdreijd@gmail.com (D.J. van der Reijd).

https://doi.org/10.1016/j.clinimag.2025.110417
Received 12 September 2024; Received in revised form 16 January 2025; Accepted 26 January 2025
Available online 27 January 2025

sensitivity for detecting CRLM, due to the introduction of diffusion weighted imaging (DWI) and hepatocyte-specific contrast agents.[5,6] Gadoxetic acid is a hepatocyte specific contrast agent, sold under the brand of Eovist/Primovist® (Bayer Pharmaceuticals, Berlin), and behaves similar to traditional extracellular gadolinium initially after injection. The excretion route is different; whereas extracellular gadolinium has renal excretion, 50 % of gadoxetic acid is absorbed by the hepatocytes. This results in peak enhancement of the liver parenchyma 20 min into the hepatobiliary phase.[7,8] This late phase provides high conspicuity of CRLM and gives an overview of the anatomy of the bile ducts, which is particularly beneficial for patients considered for local treatment.[9]

After chemotherapy treatment, the superiority of MRI compared to CT in detecting CRLM increases compared to the baseline setting.[10] This is mainly due to parenchymal changes caused by chemotherapy toxicity, such as steatosis. In some patients, the parenchymal enhancement on CT decreases, resulting in a lower lesion-to-liver contrast and thus a reduced accuracy for detection of CRLM.[11,12] Cellular changes caused by chemotherapy not only alter the liver parenchyma itself, but also influence the imaging characteristics of the CRLM, which makes characterization and reporting after chemotherapy more challenging.

Imaging characteristics of CRLM have mainly been described for MRI acquired using extracellular gadolinium contrast agents and before the onset of systemic treatment. Typical characteristics include hypovascularity, arterial rim enhancement and diffusion restriction.[13,14] However, there is a rise in the use of gadoxetic acid-enhanced MRI and (neo)adjuvant systemic treatment. Therefore, the aim of this study is to determine to what extent these typical MRI characteristics of CRLM occur on gadoxetic acid-enhanced MRI, and persist after chemotherapy.

2. Methods

2.1. Study population

This retrospective, single-centre study was approved by our institutional review board (IRBd20–189) and informed consent was waived. Patients with CRLM visible on liver MRI between November 2015 and January 2021 were considered for inclusion. Patients were excluded if: (a) the MRI was acquired using extracellular contrast; (b) the diagnosis of CRLM was not confirmed by histopathology; (c) the diagnosis was mucinous adenocarcinoma as these tumors are known to display significantly distinct imaging characteristics on MRI.[15] Furthermore, CRLM were excluded if: (1) they were located next to an ablation zone, resection margin, or after stereotactic body radiation therapy (SBRT); (2) chemotherapy was administered within six months prior to MRI, as it potentially could affect the imaging characteristics; (3) no dual chemotherapy strategy (e.g. capecitabine monotherapy) was administered in the post chemotherapy analysis, since a dual strategy complies with clinical practice. Fig. 1 depicts a flowchart of the patient selection process.

2.2. MRI protocol

All MRI examinations were performed using two Philips dStream Achieva 3 T MR systems (Phillips Medical Systems International B.V., Best, The Netherlands). The imaging protocol included turbo spin echo (TSE) T2-weighted (T2W) images using MultiVane technique and respiratory triggering (repetition time/echo time (TR/TE) 2725/75 ms, slice thickness 5 mm, flip angle 90°, field of view (FOV) 400x400x233 mm^3), spin-echo echo-planar imaging (SE-EPI) DWI with b-values 0, 10,

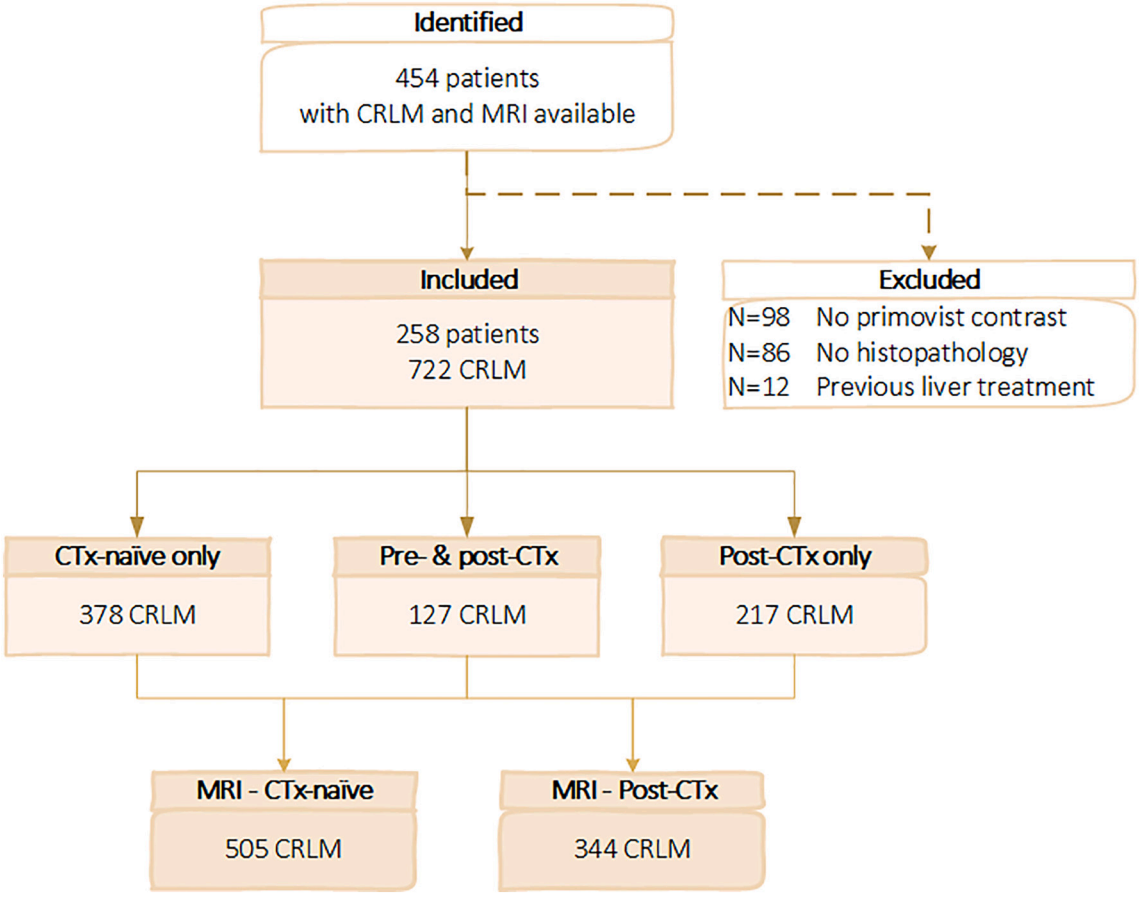

Fig. 1. Flowchart patient selection process.
Abbreviations: CRLM colorectal liver metastases, CTx chemotherapy, MRI magnetic resonance imaging.

200 and 800 s/mm^2 (TR/TE 3547/71, slice thickness 5 mm, flip angle 90°, FOV 401x450x251 mm^3), mono-exponential apparent diffusion coefficient (ADC) maps were created based on all four b-values, and breath hold T1-weighted (T1W) THRIVE images (TR/TE 3.5/1.1 ms, slice thickness 3 mm, flip angle 10°, FOV 296x400x212 mm^3) including in-phase, out-phase and fat suppressed images. This was followed by the injection of 10 ml gadoxetic acid by an injector at a fixed rate of 3 ml/s and followed by a flush of 30 ml saline. The dynamic contrast enhanced (CE-) images were acquired in the arterial phase at 25 s post injection (p.i.), portal venous phase (60 s p.i.), transitional phase (180 s p.i.) and hepatobiliary phase (20 min p.i.). Post-chemotherapy MRI was acquired after at least three cycles of a 3-weekly chemotherapeutic agent, or four cycles of a 2-weekly chemotherapeutic agent.

2.3. Lesion selection

At least one CRLM per patient was proven with histopathology. Lesions without histopathology were considered CRLM if: 1) lesions showed size reduction during chemotherapy; 2) lesions showed growth over time; or 3) if lesions had comparable imaging characteristics as the lesion with histopathology. For patients with multiple metastases, a maximum of five CRLM were randomly selected. No size cut-offs were applied.

2.4. Image assessment

All MRIs were retrospectively reassessed by one of the two dedicated abdominal radiologists (ES or BH) with 7 or 16 years of experience in liver imaging, who were blinded to the patient characteristics. The assessed sequences included the unenhanced (UE-) T1W images, the CE-T1W images combining the arterial and portal venous phase, the T1W hepatobiliary phase, the T2W images, the DWI with b value 800 s/mm^2 and corresponding ADC map. The included lesions were scored with the use of a scoring list developed for the purpose of this study. Fig. 2 shows the scoring options with examples per sequence. The characteristics considered as typical (highlighted yellow in Fig. 2) were: 1) non-enhanced T1W hypointensity; 2) hypovascular; 3) arterial rim enhancement; 4) non-enhancing in the hepatobiliary phase compared to the liver parenchyma; 5) T2W mild hyperintensity; and 6) diffusion restriction.[13,16] All characteristics were qualitatively assessed. The largest diameter in millimeters (mm) was measured in the hepatobiliary phase. If a sequence was of unsatisfactory quality, it was marked as "quality lacking", and the lesion was excluded from analysis for that specific sequence. Also, lesions not visible on a specific sequence post-chemotherapy were likewise excluded from analysis for that specific sequence.

2.5. Analysis

Descriptive statistics were used to present the findings, for which the Statistical Package for the Social Sciences (SPSS, version 29.0; SPSS, Chicago) was used. The mean and standard deviation were reported for continuous variables. Categorical variables were expressed in terms of frequencies and percentages. Correlations between categorical outcomes were calculated with the Chi-square statistic.

3. Results

3.1. Patient and lesion characteristics

258 patients with 722 unique CRLM were included for analysis. Patient characteristics are presented in Table 1. 127 CRLM had both a pre- and post-chemotherapy MRI available and were scored twice on different time points. 473 CRLM (66 %) were located in the right liver lobe, 239 CRLM (33 %) in the left liver lobe, and 10 CRLM were located in the caudate lobe (1 %).

3.2. Chemotherapy-naïve CRLM

505 chemotherapy-naive CRLM were assessed with a median size of 16 mm (range 3–173 mm, interquartile range (IQR) 11–25 mm). 249 CRLM (49 %) showed all the six predefined typical imaging characteristics and all CRLM showed at least two typical imaging characteristics (Table 2). An example of a CRLM with atypical characteristics is displayed in Fig. 3, and a CRLM with typical characteristics is displayed in Fig. 4. On the UE-T1W images 96 % of the lesions appeared hypointense and 4 % of the lesions appeared isointense. 98 % of CRLM were assessed as hypovascular and 2 % as hypervascular on the CE-T1W images. The pattern of enhancement was arterial rim in 58 % of CRLM, homogeneous in 29 %, and heterogeneous in 13 %. In the hepatobiliary phase, all 505 CRLM appeared non-enhancing compared to the liver parenchyma. On the T2W images, 95 % of CRLM appeared mildly hyperintense, 5 % isointense, and 1 CRLM strongly hyperintense (0.2 %). Diffusion restriction was found in 88 % of CRLM.

3.3. Post-chemotherapy CRLM

344 CRLM were assessed post-chemotherapy and showed a median size of 12 mm (range 2–130 mm, IQR 8–20 mm). All six typical characteristics were present in 87/344 CRLM (25 %) and 52/344 CRLM (16 %) showed ≤3 typical characteristics (Table 2). On the UE-T1W images, 93 % appeared hypointense. The vascularity was assessed as hypovascular in 99.7 %. The pattern of enhancement on the CE-T1W images was arterial rim in 51 %, homogeneous in 41 %, and heterogeneous in 8 %. All CRLM were non-enhancing in the hepatobiliary phase. On the T2W images 79 % appeared mildly hyperintense, 20 % appeared isointense, and 1 CRLM appeared strongly hyperintense (0.3 %). 65 % of CRLM presented diffusion restriction. Diffusion restriction and T2W appearance were correlated, with 68 % of CRLM with T2W isointensity lacking diffusion restriction, compared to 28 % of CRLM appearing mildly hyperintense on T2W images ($p < 0.001$).

3.4. Pre- and post-chemotherapy MRI

127 CRLM were assessed both pre- and post-chemotherapy. The mean time between the two MRIs was 134 ± 65 days. The mean size pre-chemotherapy was 22 ± 13 mm and a median decrease in size of 8 mm (range − 45 to +13 mm) was found post-chemotherapy. In this subgroup, the occurrence of arterial rim enhancement decreased after chemotherapy from 85 % to 51 % and the enhancement pattern shifted to more homogeneous enhancement (8 % vs 38 %; pre- and post-chemotherapy, respectively). On T2W pre- and post-MRI, the majority of the CRLM appeared mildly hyperintense (94 % and 75 %, respectively). However, 21 % of CRLM appearing mildly hyperintense pre-chemotherapy became isointense post-chemotherapy. All lesions with T2W isointensity on pre-MRI remained isointense on post-MRI. Furthermore, 32 % of CRLM exhibiting diffusion restriction on the pre-MRI lost this characteristic on the post-MRI, while all CRLM ($n = 11$) without diffusion restriction on pre-MRI remained without on the post-MRI. An example of a CRLM with typical imaging characteristics and its changes post-chemotherapy is depicted in Figs. 4 and 5.

4. Discussion

This study investigated the occurrence of typical characteristics of CRLM on gadoxetic acid-enhanced MRI in a large cohort before and after chemotherapy. The appearance of CRLM has mainly been described before chemotherapy treatment and with the use of non-hepatocyte specific contrast agents. In the current paper only 49 % of the chemotherapy-naïve CRLM showed all typical characteristics, and post-chemotherapy all typical characteristics appeared in only 25 % of CRLM. Specifically, the occurrence of arterial rim enhancement, mild T2W hyperintensity, and diffusion restriction was less frequently found

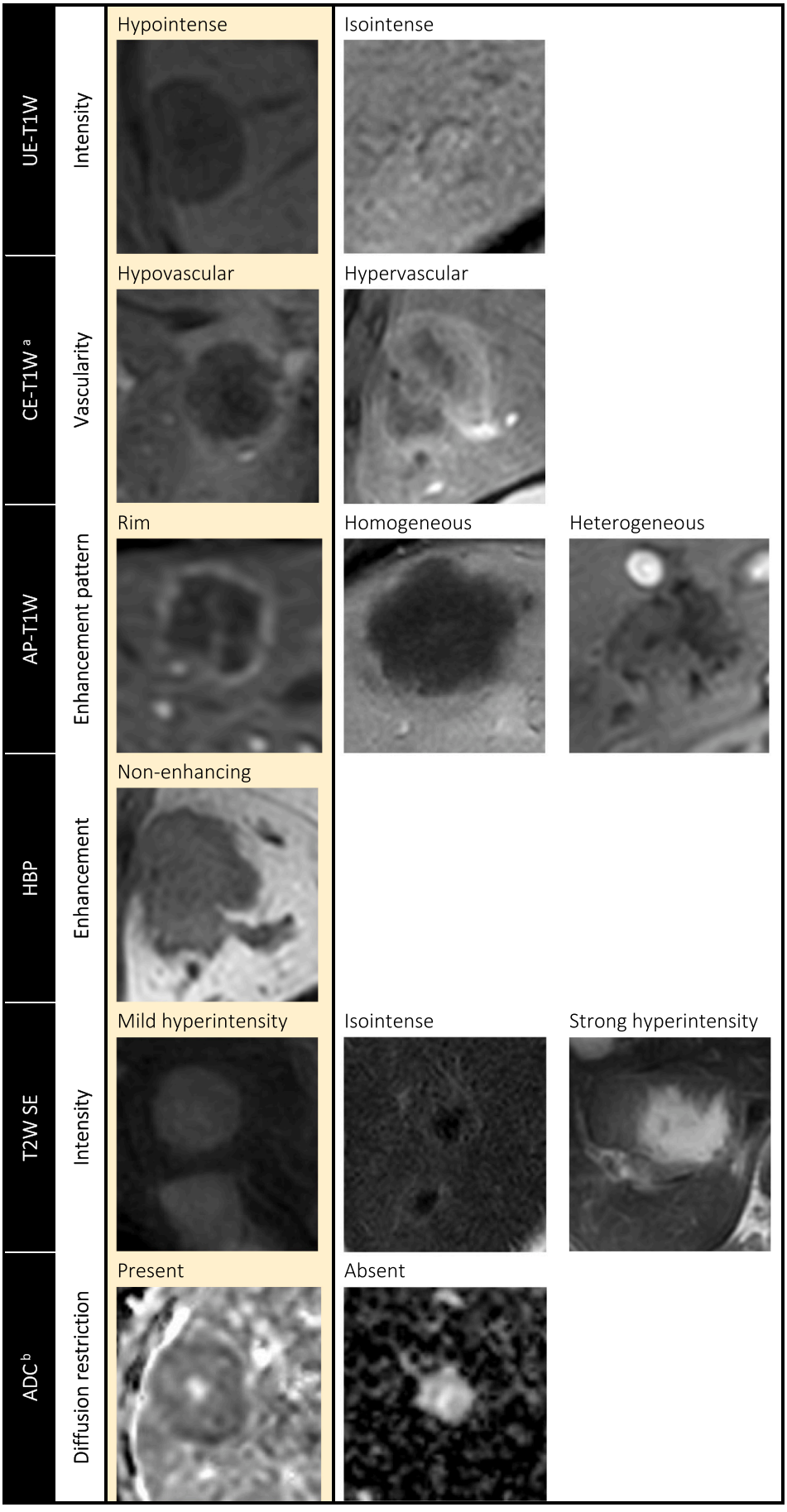

(caption on next page)

Fig. 2. Imaging characteristics scored per sequence.
Abbreviations: ADC apparent diffusion coefficient, AP arterial phase, CE contrast-enhanced, DWI diffusion weighted imaging, HBP hepatobiliary phase, SE short echo time, UE unenhanced.
[a]For assessment of vascularity, both the arterial and portal venous phase images were evaluated.
[b]For assessment of diffusion restriction, both DWI and the ADC map were evaluated.

on the post-chemotherapy MRI. This paper is meant to familiarize radiologists with these findings.

Arterial rim enhancement is related to the vascularization and perfusion of the tumor-to-liver border.[17] Previous research has shown that arterial rim enhancement only minimally reflects the periphery of the tumor, and mainly displays extra-tumoural parenchymal changes like inflammatory infiltration, vascular proliferation and/or a desmoplastic reaction.[18–20] We found that 58 % of chemotherapy-naïve CRLM showed arterial rim enhancement and 51 % post-chemotherapy, which is in line with an earlier study on gadoxetic acid-enhanced MRI that found an arterial rim in 41 % of the CRLM. Studies analyzing CRLM with extracellular gadolinium contrast agents found that 68 %–74 % of CRLM show arterial rim enhancement.[17,18] This suggests that the hepatocyte specific contrast agents could lead to less arterial rim enhancement, but head-to-head comparison is lacking. Li et al proposed that peripheral rim enhancement depends on the histopathological growth pattern (HGP): in their study 100 % of CRLM with a replacement-HGP showed rim enhancement compared to only 46 % of the CRLM that had a non-replacement-HGP.[17] On CE-CT the presence of peripheral rim enhancement after chemotherapy was found to be related to responses predominated by necrosis rather than fibrosis, and also with histologic presence of viable tumor cells.[21,22] This might explain the slight decrease in occurrence of arterial rim enhancement after chemotherapy in our study. Additionally, we found more CRLM appeared homogeneous after chemotherapy compared to the chemotherapy-naïve lesions (41 % vs 29 %, respectively). This was expected as chemotherapy induces necrosis which leads to a decrease in contrast entering the CRLM, resulting in a more homogeneous aspect.[23]

CRLM are known to exhibit diffusion restriction, meaning the free movement of water molecules is restricted, resulting in high signal on DWI with corresponding low ADC values. The reduced ADC values in malignant tumors is attributed to multiple factors, including the size and viscosity of the extracellular space, increased cellularity and disorganization of cells.[24–26] In our study, 12 % of chemotherapy-naïve CRLM, and 35 % post-chemotherapy did not exhibit diffusion restriction. Post-chemotherapy, the absence of diffusion restriction is probably caused by decreased cellularity due to chemotherapy induced apoptosis, creating more space for water molecules to move. Additionally, previous research had indicated lower reliability for ADC values after treatment and reduced accuracy in detecting CRLM using DWI.[24,27,28] The absence of diffusion restriction in chemotherapy-naïve CRLM are in contrast with earlier findings of Granata et al, who described that all included untreated CRLM showed diffusion restriction.[16] Although this difference

Table 1
Patient characteristics.

Baseline characteristics	N = 258 patients
Age[a] (years)	62 ± 11
Sex (%)	
Female	101 (39)
Male	157 (61)
Location primary tumor (%)	
Right sided colon	46 (18)
Left sided colon	122 (47)
Rectum	90 (35)
T-stage primary tumor (%)	
T1	9 (3)
T2	25 (10)
T3	165 (64)
T4	54 (21)
Unknown	5 (2)
N-stage primary tumor (%)	
N0	84 (33)
N+	170 (66)
Unknown	4 (1)
Timing of CRLM (%)	
Synchronous (<6 months)	165 (64)
Metachronous (>6 months)	93 (36)
Histopathology acquired by (%)	
Resection	231 (90)
Biopsy	27 (10)
Number of CRLM assessed per patient[a]	3.4 ± 2.6

Post-chemotherapy characteristics	N = 104 patients
Chemotherapy	
Oxaliplatin-containing[b]	94 (90)
Irinotecan-containing[c]	9 (9)
Other	5 (5)
Monoclonal antibodies treatment	
Bevacuzimab	69 (66)
Panitumumab	5 (5)
Cetuximab	1 (1)
None	29 (28)

Abbreviations: N number, CRLM colorectal liver metastases, T-stage tumor stage, N-stage nodal stage.
[a] numerical variables are expressed as mean with a standard deviation.
[b] Combined with either Capecitabine (CAPOX) or 5-Fluorouracil/leucovorin (FOLFOX), without or with Irinotecan (FOLFOXIRI).
[c] Combined with 5-Fluorouracil/leucovorin (FOLFIRI), either without or with oxaliplatin (FOLFOXIRI).

Table 2
Distribution of imaging characteristics of CRLM per subgroup.

	CTx-naïve CRLM n = 505[a] (%)	Post-CTx CRLM n = 344[a] (%)
UE-T1W intensity		
Hypointensity	485 (96)	311 (93)
Isointensity	20 (4)	25 (7)
CE-T1W vascularity		
Hypovascular	495 (98)	330 (100)
Hypervascular	9 (2)	1 (0)
AP-T1W enhancement		
Arterial rim	291 (58)	154 (51)
Homogeneous	144 (29)	122 (41)
Heterogeneous	63 (13)	25 (8)
Hepatobiliary phase		
Non-enhancing	505 (100)	306 (100)
T2W-SE		
Mild hyperintensity	478 (95)	269 (79)
Isointensity	26 (5)	69 (21)
Strong hyperintensity	1 (0)	1 (0)
Diffusion restriction		
Present	435 (87)	200 (65)
Absent	62 (13)	106 (35)
Distribution of typical characteristics		
1 typical characteristic	0 (0)	2 (1)
2 typical characteristics	4 (1)	10 (3)
3 typical characteristics	15 (3)	40 (12)
4 typical characteristics	36 (7)	79 (23)
5 typical characteristics	201 (40)	126 (36)
6 typical characteristics	249 (49)	87 (25)

Abbreviations: CRLM colorectal liver metastases, CT chemotherapy, UE unenhanced, T1W T1-weighted, CE contrast-enhanced, AP arterial phase, T2W-SE T2-weighted short echo time.
[a] Invisible CRLM or CRLM visualized on sequences with unsatisfactory quality, were excluded for analysis for this specific sequence.

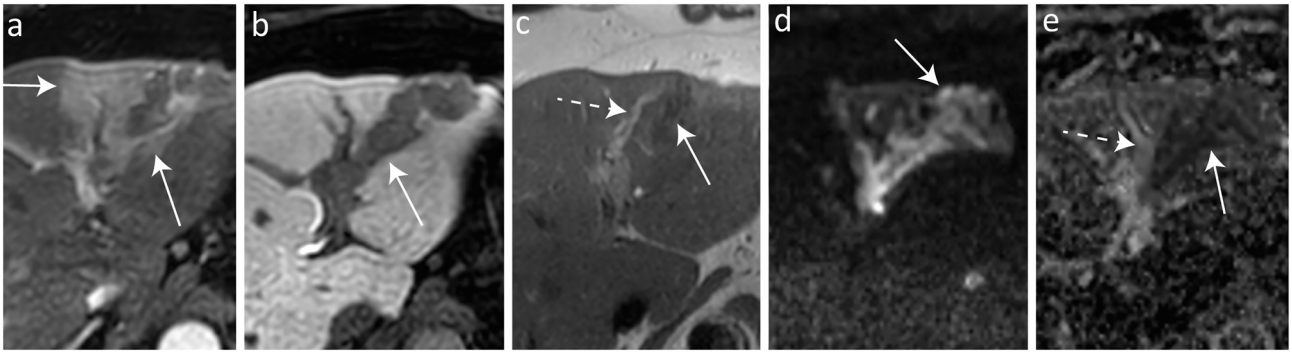

Fig. 3. Example atypical CRLM.
A chemotherapy-naïve CRLM with atypical characteristics: a hypovascular lesion with thick rim enhancement in the arterial phase (a), the hepatobiliary phase shows the lesion is more narrow than expected and wedge shaped (b). On the T2W images (c), the lesion is mostly isointense (full arrow) with a mild hyperintense border on the lateral side (dashed arrow). A scattered high signal is found on the DWI (d), corresponding with a low signal (full arrow) on the ADC map (e), with T2W shine through lateral to the lesion (dashed arrow). Cholangiocarcinoma was considered as a differential diagnosis, but biopsy showed histopathology corresponding to CRLM.

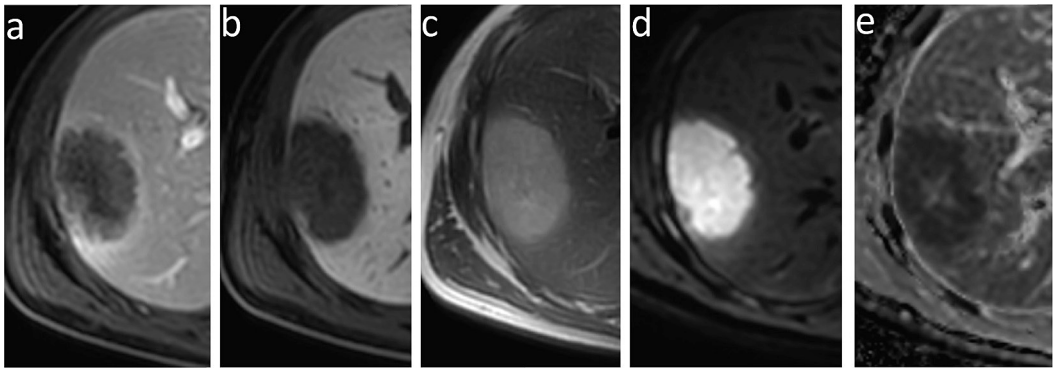

Fig. 4. Example typical CRLM pre-chemotherapy.
A CRLM showing all 6 typical characteristics on pre-chemotherapy MRI: a hypovascular lesion with rim enhancement on the arterial phase (a), is non-enhancing in the hepatobiliary phase (b), mildly hyperintense on the T2W images (c), shows high signal on the b800 DWI (d) with low signal on the ADC (e) corresponding to diffusion restriction.

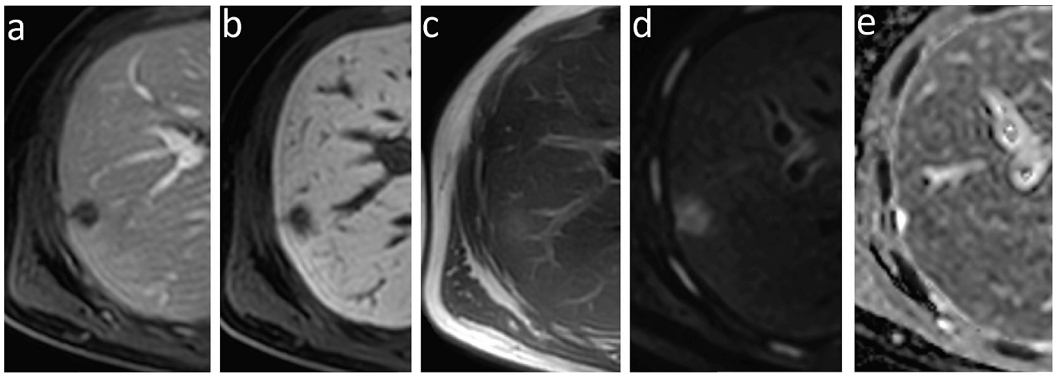

Fig. 5. Example CRLM changes post-chemotherapy.
The lesion from Fig. 4 post-chemotherapy: some typical characteristics are lost, specifically no arterial rim enhancement (a) is present and there is loss of diffusion restriction (d–e). The hepatobiliary phase shows a decrease in size (b) and the lesion remains mildly hyperintense on T2W (c).

cannot be completely explained, we hypothesize it could be due to the assessment method of diffusion restriction. In our study, diffusion restriction was defined as a visually high signal on DWI accompanied by a corresponding low signal on ADC compared to the liver parenchyma. Granata et al only assessed the presence of high signal on DWI. Our results show that even if liver lesions show no diffusion restriction, the diagnosis of CRLM cannot be ruled out.

All CRLM in this study appeared non-enhancing compared to the liver parenchyma in the hepatobiliary phase. Gadoxetic acid is absorbed into the hepatocytes by OATP1 peptides for excretion through the bile.[7,29] Liver lesions originating from hepatocytes show therefore iso- or hyperintensity, such as focal nodular hyperplasia (FNH) which have increased OATP1 expression, or well-differentiated hepatocellular carcinoma (HCC) of which some maintain OATP1 expression.[29] Since CRLM lack hepatocytes gadoxetic acid is not absorbed, resulting in non-enhancement compared to the liver parenchyma. Consequently, all

CRLM in our study appeared non-enhancing in the hepatobiliary phase, regardless of whether the patients were chemotherapy-naïve or had undergone chemotherapy.

In the current study, the lack of histopathology as a ground truth for individual lesions was considered a limitation. Histopathology was available for at least one CRLM, and other lesions within the same patient with similar characteristics, lesions that grew, or lesions that responded to therapy. This selection method minimized the chance that other entities except CRLM were included, but it may have led to CRLM with atypical characteristics being missed. Also, direct comparison of MR imaging characteristics with histopathological features was not possible. This would be an interesting matter to explore in future research as it develops the knowledge on the biological background of imaging characteristics, and could help determine which imaging characteristics are related to response.

To conclude, the majority of CRLM show at least five typical imaging characteristics on gadoxetic acid-enhanced MRI. Arterial rim enhancement and diffusion restriction were not found in all chemotherapy-naïve CRLM and can therefore not be used to rule out the diagnosis. After chemotherapy, the occurrence of the typical characteristics were less frequent on gadoxetic acid-enhanced MRI, especially mild T2W hyperintensity and the presence of diffusion restriction. Knowledge among radiologists of the typical characteristics, its variations, and the changes after chemotherapy, can help in detection and reporting of CRLM.

CRediT authorship contribution statement

Denise J. van der Reijd: Writing – review & editing, Writing – original draft, Visualization, Project administration, Methodology, Formal analysis, Data curation, Conceptualization. **Ezgi A. Soykan:** Writing – review & editing, Methodology, Investigation, Formal analysis, Data curation, Conceptualization. **Birthe C. Heeres:** Methodology, Data curation. **Doenja M.J. Lambregts:** Writing – review & editing. **Marieke A. Vollebergh:** Writing – review & editing. **Koert F.D. Kuhlmann:** Writing – review & editing. **Niels F.M. Kok:** Writing – review & editing. **Petur Snaebjornsson:** Writing – review & editing. **Regina G.H. Beets-Tan:** Writing – review & editing, Supervision, Resources, Funding acquisition, Conceptualization. **Monique Maas:** Writing – review & editing, Supervision, Methodology, Investigation, Conceptualization. **Elisabeth G. Klompenhouwer:** Writing – review & editing, Writing – original draft, Supervision, Project administration, Methodology, Formal analysis, Conceptualization.

Declaration of competing interest

The authors declare that they have no known competing financial interests, or personal relationships, that could have appeared to influence the work reported in this paper.

References

1 Engstrand J, Nilsson H, Strömberg C, Jonas E, Freedman J. Colorectal cancer liver metastases - a population-based study on incidence, management and survival. BMC Cancer Jan 15 2018;18(1):78. https://doi.org/10.1186/s12885-017-3925-x.

2 Manfredi S, Lepage C, Hatem C, Coatmeur O, Faivre J, Bouvier AM. Epidemiology and management of liver metastases from colorectal cancer. Ann Surg Aug 2006;244 (2):254–9. https://doi.org/10.1097/01.sla.0000217629.94941.cf.

3 Okholm C, Mollerup TK, Schultz NA, Strandby RB, Achiam MP. Synchronous and metachronous liver metastases in patients with colorectal cancer. Dan Med J Dec 2018;65(12).

4 Van Cutsem E, Cervantes A, Adam R, et al. ESMO consensus guidelines for the management of patients with metastatic colorectal cancer. Ann Oncol Aug 2016;27 (8):1386–422. https://doi.org/10.1093/annonc/mdw235.

5 Vreugdenburg TD, Ma N, Duncan JK, Riitano D, Cameron AL, Maddern GJ. Comparative diagnostic accuracy of hepatocyte-specific gadoxetic acid (Gd-EOB-DTPA) enhanced MR imaging and contrast enhanced CT for the detection of liver metastases: a systematic review and meta-analysis. Int J Colorectal Dis Nov 2016;31 (11):1739–49. https://doi.org/10.1007/s00384-016-2664-9.

6 Choi SH, Kim SY, Park SH, et al. Diagnostic performance of CT, gadoxetate disodium-enhanced MRI, and PET/CT for the diagnosis of colorectal liver metastasis: systematic review and meta-analysis. J Magn Reson Imaging May 2018;47(5): 1237–50. https://doi.org/10.1002/jmri.25852.

7 Rybczynska D, Pienkowska J, Frydrychowski A, Szurowska E, Jankowska A. Understanding the role of gadoxetic acid in MRI. Current Medical Imaging 2020;16 (5):572–7. https://doi.org/10.2174/1573405615666181224125909.

8 Schalkx HJ, van Stralen M, Coenegrachts K, et al. Liver perfusion in dynamic contrast-enhanced magnetic resonance imaging (DCE-MRI): comparison of enhancement in Gd-BT-DO3A and Gd-EOB-DTPA in normal liver parenchyma. Eur Radiol Sep 2014;24(9):2146–56. https://doi.org/10.1007/s00330-014-3275-x.

9 Görgec B, Hansen IS, Kemmerich G, et al. MRI in addition to CT in patients scheduled for local therapy of colorectal liver metastases (CAMINO): an international, multicentre, prospective, diagnostic accuracy trial. Lancet Oncol Dec 8 2023. https://doi.org/10.1016/s1470-2045(23)00572-7.

10 Jhaveri KS, Fischer SE, Hosseini-Nik H, et al. Prospective comparison of gadoxetic acid-enhanced liver MRI and contrast-enhanced CT with histopathological correlation for preoperative detection of colorectal liver metastases following chemotherapy and potential impact on surgical plan. HPB Nov 2017;19(11): 992–1000. https://doi.org/10.1016/j.hpb.2017.06.014.

11 van Kessel CS, Buckens CF, van den Bosch MA, van Leeuwen MS, van Hillegersberg R, Verkooijen HM. Preoperative imaging of colorectal liver metastases after neoadjuvant chemotherapy: a meta-analysis. Ann Surg Oncol Sep 2012;19(9): 2805–13. https://doi.org/10.1245/s10434-012-2300-z.

12 Angliviel B, Benoist S, Penna C, et al. Impact of chemotherapy on the accuracy of computed tomography scan for the evaluation of colorectal liver metastases. Ann Surg Oncol May 2009;16(5):1247–53. https://doi.org/10.1245/s10434-009-0385-9.

13 Danet IM, Semelka RC, Leonardou P, et al. Spectrum of MRI appearances of untreated metastases of the liver. AJR Am J Roentgenol Sep 2003;181(3):809–17. https://doi.org/10.2214/ajr.181.3.1810809.

14 Campos JT, Sirlin CB, Choi JY. Focal hepatic lesions in Gd-EOB-DTPA enhanced MRI: the atlas. Insights Imaging Oct 2012;3(5):451–74. https://doi.org/10.1007/s13244-012-0179-7.

15. Granata V, Fusco R, De Muzio F, et al. Magnetic resonance features of liver mucinous colorectal metastases: what the radiologist should know. J Clin Med. Apr 15 2022;11 (8)doi:https://doi.org/10.3390/jcm11082221.

16 Granata V, Catalano O, Fusco R, et al. The target sign in colorectal liver metastases: an atypical Gd-EOB-DTPA "uptake" on the hepatobiliary phase of MR imaging. Abdom Imaging Oct 2015;40(7):2364–71. https://doi.org/10.1007/s00261-015-0488-7.

17 Li WH, Wang S, Liu Y, Wang XF, Wang YF, Chai RM. Differentiation of histopathological growth patterns of colorectal liver metastases by MRI features. Quant Imaging Med Surg Jan 2022;12(1):608–17. https://doi.org/10.21037/qims-21-143.

18 Yu JS, Rofsky NM. Hepatic metastases: perilesional enhancement on dynamic MRI. AJR Am J Roentgenol Apr 2006;186(4):1051–8. https://doi.org/10.2214/ajr.04.1698.

19 Semelka RC, Hussain SM, Marcos HB, Woosley JT. Perilesional enhancement of hepatic metastases: correlation between MR imaging and histopathologic findings-initial observations. Radiology Apr 2000;215(1):89–94. https://doi.org/10.1148/radiology.215.1.r00mr2989.

20 Namasivayam S, Martin DR, Saini S. Imaging of liver metastases: MRI. Cancer Imaging 2007;7(1):2–9. https://doi.org/10.1102/1470-7330.2007.0002.

21 Ishida K, Tamura A, Kato K, et al. Correlation between CT morphologic appearance and histologic findings in colorectal liver metastasis after preoperative chemotherapy. Abdominal Radiology (New York) Nov 2018;43(11):2991–3000. https://doi.org/10.1007/s00261-018-1588-y.

22 Serrablo A, Paliogiannis P, Paradisi C, et al. Radio-pathological correlations in patients with liver metastases for colorectal cancer. Dig Surg 2020;37(5):383–9. https://doi.org/10.1159/000506105.

23 Maclean D, Tsakok M, Gleeson F, et al. Comprehensive imaging characterization of colorectal liver metastases. Front Oncol 2021;11:730854. https://doi.org/10.3389/fonc.2021.730854.

24 Padhani AR, Liu G, Koh DM, et al. Diffusion-weighted magnetic resonance imaging as a cancer biomarker: consensus and recommendations. Neoplasia (New York, NY) Feb 2009;11(2):102–25. https://doi.org/10.1593/neo.81328.

25. Kele PG, van der Jagt EJ. Diffusion weighted imaging in the liver. World J Gastroenterol. Apr 7 2010;16(13):1567–76. doi:https://doi.org/10.3748/wjg.v16.i13.1567.

26 Vu LN, Morelli JN, Szklaruk J. Basic MRI for the liver oncologists and surgeons. Journal of Hepatocellular Carcinoma 2017;5:37–50. https://doi.org/10.2147/jhc.S154321.

27 Yu MH, Lee JM, Hur BY, et al. Gadoxetic acid-enhanced MRI and diffusion-weighted imaging for the detection of colorectal liver metastases after neoadjuvant chemotherapy. Eur Radiol Aug 2015;25(8):2428–36. https://doi.org/10.1007/s00330-015-3615-5.

28 Macera A, Lario C, Petracchini M, et al. Staging of colorectal liver metastases after preoperative chemotherapy. Diffusion-weighted imaging in combination with Gd-EOB-DTPA MRI sequences increases sensitivity and diagnostic accuracy. Eur Radiol Mar 2013;23(3):739–47. https://doi.org/10.1007/s00330-012-2658-0.

29 Van Beers BE, Pastor CM, Hussain HK. Primovist, Eovist: what to expect? J Hepatol Aug 2012;57(2):421–9. https://doi.org/10.1016/j.jhep.2012.01.031.